CHAPTER 8

MOLAR MASS DEPENDENT GROWTH OF POLY(ε-CAPROLACTONE) CRYSTALS IN LANGMUIR FILMS

Reproduced with permission from: **Li, B.**; Esker, A. R. "Molar Mass Dependent Growth of Poly(ε-caprolactone) Crystals in Langmuir Films," *Langmuir*, **2007**, *23*, 2546.

8.1. Abstract

Poly (ε-caprolactone) (PCL) samples with weight average molar masses (M_w) ranging from 5.2 to 42.8 kg·mol^{-1} exhibit molar mass dependent nucleation and growth of crystals, crystal morphologies, and melting properties at a temperature of 22.5 °C in Langmuir films at the air/water (A/W) interface. At surface areas per monomer, A, greater than ~ 37 Å^2·monomer^{-1}, surface pressure, Π, and surface elasticity exhibit molar mass independent behavior that is consistent with a semi-dilute PCL monolayer. In this regime, the scaling exponent indicates that the A/W interface is a good solvent for the liquid-expanded PCL monolayers. Π-A isotherms show molar mass dependent behavior in the vicinity of the collapse transition, i.e. the supersaturated monolayer state, corresponding to the onset of the nucleation of crystals. Molar mass dependent morphological features for PCL crystals and their subsequent crystal melting are studied by *in situ* Brewster angle microscopy (BAM) during hysteresis experiments. The competition between lower segmental mobility and a greater degree of undercooling with increasing molar mass produces a maximum average growth rate at intermediate molar

mass. This behavior is analogous to spherulitic growth in bulk PCL melts. The plateau regions in the expansion isotherms represent the melting process, where the polymer chains continuously return to the monolayer state. The magnitude of Π for the plateau during expansion decreases with increasing molar mass, indicating that the melting process is strongly molar mass dependent.

8.2. Introduction

Poly (ε-caprolactone) (PCL) is a semicrystalline polyester with a bulk glass transition temperature (T_g) of ~ -60 °C, a low melting temperature (T_m) of ~ 50 °C, excellent biocompatibility, and low toxicity. In the past decade, PCL has been considered as a model system for investigating the crystallization of polymer confined in thin or ultrathin films.[8-10] It is well-known that the confinement of semicrystalline polymers in thin films can significantly alter properties such as molecular mobility,[4, 5] the glass transition temperature,[6, 7] chain orientation,[145] etc. For instance, the interfacial interactions between films and substrates may alter the transport properties of polymer molecules to the growth fronts of crystallizing lamellae, thereby altering growth rates, morphologies, and melting temperatures for crystals grown in thin films.[8-23]

Previous studies of PCL crystallization in PCL/polyvinyl chloride spincoated films[8, 10] reveal that isothermal crystallization rates decrease when the film thickness is less than 1 μm. A decrease in the isothermal crystallization rate was also observed for pure PCL crystallized in spincoated films with thicknesses less than 30 nm.[9] For example, the growth rate is about one-half the bulk growth rate at crystallization temperatures of 50 °C and 54 °C for 15 nm thick films; while for 6 nm thick films, the growth rate decreases dramatically, resulting in a growth rate that is similar at both temperatures. In contrast,

growth rates observed for PCL films with thicknesses in the range of 30 to 200 nm at both 50 °C and 54 °C are consistent with measurements for thicker films up to 2000 nm and bulk crystallization. Comparable results have also been reported for poly (di-n-hexysilane), isotactic-polystyrene, and poly(ethylene oxide).[203, 122, 11-16] In addition, nonlinearity of the isothermal crystallization rates is ultimately observed for 15 nm and 6 nm thick PCL films after a sufficient period of growth.[9] All of these studies indicate that the diffusion of polymer chains from the surrounding melt to the growth front becomes a determining factor for crystal growth in two-dimensional (2D) constrained geometries as the film thickness decreases below a certain threshold thickness value.[8-23] As a consequence, typical diffusion-limited growth morphologies are observed in sufficiently thin films for different polymers. One pertinent example for this study is the dendritic growth observed in 6 nm or thinner PCL films spincoated onto silicon substrates.[9]

For the aforementioned studies, thin films of PCL or its blends are usually prepared on solid substrates by spincoating and the film thicknesses are controlled by varying the concentration of the polymer solution or the spinning rate. On solid substrates, the cooperative movements of polymer chains directly affects chain folding and consequently the crystallization rate and morphology. Furthermore, surface defects on solid substrates can affect the nucleation and growth mechanism for crystal growth. At the air/water (A/W) interface, the ultrapure water minimizes surface defects, providing a model surface for probing crystallization in thin films. In addition, PCL Langmuir films formed at low surface pressures are very uniform approaching monomer thickness.[24] Hence, Langmuir films represent the thinnest possible uniform film for PCL.[24] Brewster angle microscopy (BAM) studies, performed simultaneously during hysteresis experiments, allow us to

monitor the *in situ* morphologies of crystal growth and melting in Langmuir films. Moreover, the lateral force applied to Langmuir films during compression may influence molecular diffusion, and the nucleation and growth of crystals in thin films. Therefore, Langmuir films offer an opportunity to obtain a fundamental understanding of polymer crystallization in uniform monolayers and may even be extended to studies of polymer crystallization in "2D" confined systems with applied shear forces.

In Chapter 4, we reported the isothermal crystallization behavior of PCL (weight average molar mass, M_w = 10 kg·mol^{-1}, T = 22.5 °C) in Langmuir monolayers at the A/W interface.[31] Nucleation occurs in a meta-stable ("supercooled") monolayer just below the dynamic collapse pressure of $\Pi_C \sim 11$ mN·m^{-1}. Both crystal growth and melting of PCL crystals were observed by *in situ* BAM studies. Electron diffraction studies on Langmuir-Schaefer films suggest that the lamellar crystals are oriented with the polymer chain axes perpendicular to the substrate surface, while atomic force microscopy (AFM) reveals a crystal thickness of ~ 8 nm.

Moreover, PCL, as a model system for studying polymer crystallization in Langmuir films at the A/W interface, opens up the possibility of exploring many unresolved issues. Some of these are how molar mass affects the nucleation, growth, growth rate, morphology, and melting of PCL crystals in Langmuir films. It is well-known that molar mass, a key factor for determining polymer chain mobility, polymer viscosity, and melting temperature, can dramatically affect the degree of crystallinity, crystallization rate, and crystal morphology in polymer systems through the interplay between the degree of undercooling and the diffusion characteristics of the polymer.[76] Recent widespread interest in the study of PCL crystallization comes from its potential biomedical

applications in tissue engineering[154-162] and drug delivery systems,[151-153] where biodegradability is directly related to crystallinity.[76] In addition, if one considers the presence of hydrophilic/hydrophobic interfaces in many biological systems, where the biodegradation of PCL occurs, studies of molar mass dependent PCL crystal growth in Langmuir films at the A/W interface take on added relevance and may provide valuable information to guide potential biomedical applications. To the best of our knowledge, studies of molar mass dependent crystal growth for PCL in Langmuir films have not been previously reported.

In this study, isothermal crystallization and melting of PCL samples with M_w ranging from 5.2 to 42.8 kg·mol^{-1} were studied in real time by BAM. Surface pressure - area per repeat unit (or monomer for short, Π-A) isotherms for PCL are discussed in terms of their molar mass dependent phase behavior. Growth rates of PCL with various molar masses in Langmuir films are compared to previous results obtained for bulk crystallization. This study provides a detailed examination on how polymer molar mass affects the nucleation, growth rate, morphology, and melting of PCL crystals in Langmuir films at the A/W interface during compression and expansion of the films.

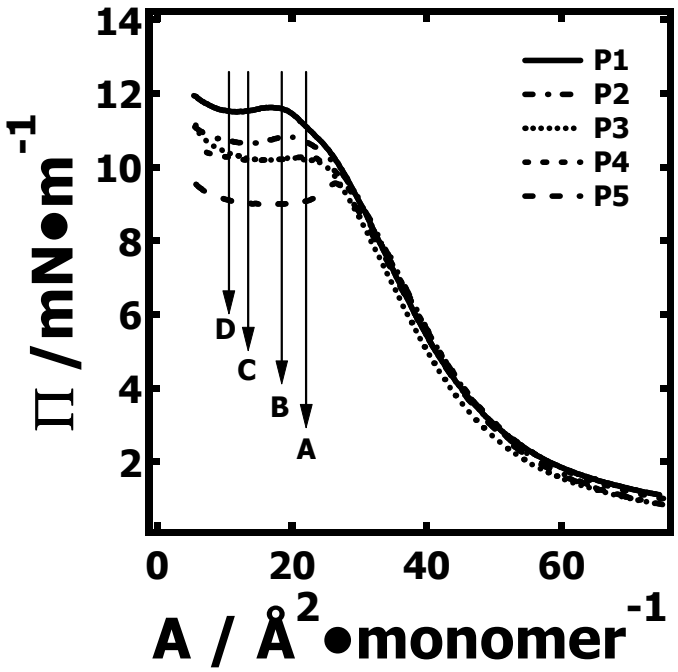

Figure 8.1. Π-A isotherms for PCL samples with different molar masses. The experiments were performed at T = 22.5 °C by compression at a constant compression rate of 8 $cm^2 \cdot min^{-1}$. P1, P2, P3, P4, and P5 correspond to M_w = 5.2, 10, 13, 15.5, and 42.8 $kg \cdot mol^{-1}$, respectively. The letters on the graph show the positions where a series of BAM images in Figure 8.6 were taken.

8.3. Results and Discussion

8.3.1. Compression Π-A Isotherms for A ≥ 52 $Å^2 \cdot monomer^{-1}$

Figure 8.1 shows a plot of surface pressure, Π, as a function of area per monomer, A, for PCL samples with different molar masses. The isotherms for all PCL samples are considered on the repeating unit ("monomer" for short) basis, regardless of the full length of each chain. The limiting areas for the five samples, obtained by extrapolating the

steepest part of each isotherm back to the A-axis, are almost identical at $A_0 \sim 52$ Å^2·monomer^{-1}. For all PCL samples at A > ~ 52 Å^2·monomer^{-1}, Π increases slowly with increasing surface concentration. The ester linkages in the polymer backbones are likely adsorbed to the water subphase, and the hydrophobic alkyl portion of the repeating unit, $(CH_2)_5$, makes PCL amphiphilic enough to remain at the A/W interface.[24]

Esker *et al.* showed that the traditional approach for describing the scaling behavior of Π with respect to surface concentration, Γ = 1/A, i.e. $\Pi \propto \Gamma^z$, in the semi-dilute regime, could be reduced to Eqs. 8-1 and 8-2 if one assumes that Π = 0 at the onset of semi-dilute monolayer regime.[56]

$$\Pi = CA^{-z} \tag{8-1}$$

$$\varepsilon_s = z\Pi \tag{8-2}$$

In this treatment, z, the two-dimensional scaling exponent, has a value of $z = 2.86$ for a good solvent,[171] and values ranging from 8 to 101 for theta solvent conditions depending on the theoretical treatment used to obtain z.[172, 173] For comparison, mean field treatments yield $z = 3$ (good solvent) and $z \to \infty$ (theta solvent).[172] The static dilational elasticity, ε_s, the quasi-2D analog of the bulk modulus, is defined as

$$\varepsilon_S = \kappa^{-1} = -A\left(\frac{\partial \Pi}{\partial A}\right)_T \tag{8-3}$$

where κ is the 2D-analog of the bulk isothermal compressibility. Using the Π-A isotherm data in Figure 8.1, ε_s is plotted as a function of Π in Figure 8.2. As seen in Figure 8.2, ε_s scaling with Π is in excellent agreement with good solvent conditions for all five PCL samples. The observation of molar mass independent behavior at Π < 4 mN·m^{-1} is consistent with the predictions of scaling theory associated with chain conformations and

polymer-solvent interactions where the monolayer can be thought of as a 2D semi-dilute solution. This approach for analyzing the data is in accordance with previous studies of other polymer monolayers at the A/W interface.[169, 170] Hence, the A/W interface can be regarded as a good solvent for PCL. For all samples at $\Pi < \sim 2$ mN·m^{-1} ($A > \sim 52$ Å^2·monomer^{-1}), ε_s is very small, indicating large κ in this regime. The large observed κ suggests a significant amount of water is bound to the hydrophilic groups.

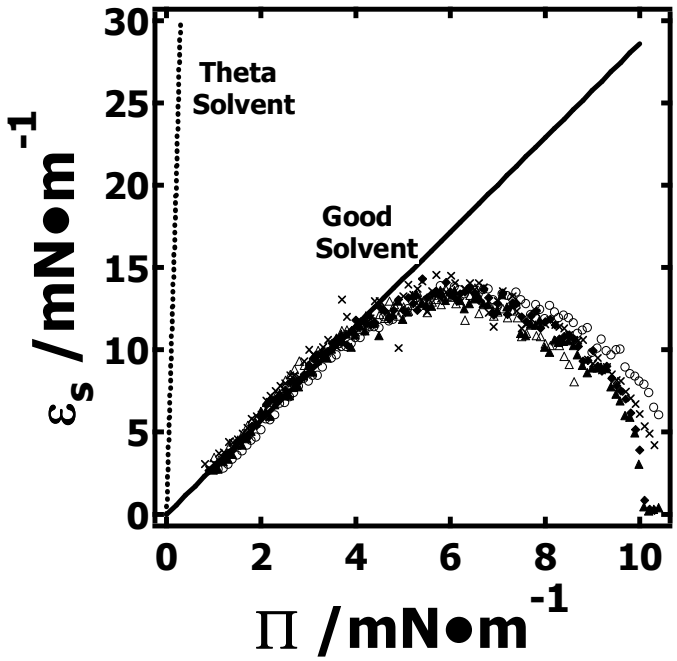

Figure 8.2. ε_s vs. Π for PCL samples with different molar masses. The symbols correspond to M_w = 5.2 (P1, ○), 10 (P2, ×), 13 (P3, ♦), 15.5 (P4, ▲), and 42.8 (P5, Δ) kg·mol^{-1}. The lines are theoretical curves, $\varepsilon_s = z\Pi$, for good solvent conditions (z = 2.86, solid line)[171] and the most extreme value reported for theta solvent conditions (z = 101, dotted line).[172]

8.3.2. Compression Π-A Isotherms for 37 < A < ~ 52 Å^2·monomer^{-1}

Continuing with the discussion of Figure 8.1, upon further compression of the monolayer, at ~ 37 < A < ~ 52 Å^2·monomer^{-1}, Π increases more quickly than for A > ~ 52 Å^2·monomer^{-1}, indicating that the 2D compressibility of the monolayers is decreasing. In order to quantitatively understand the changing slope in Figure 8.1 for 37 < A < ~ 52 Å^2·monomer^{-1}, ε_s is also plotted as a function of A in Figure 8.3. As seen in Figure 8.3, ε_s rises with decreasing A until a molar mass independent maximum, $\varepsilon_{s,max}$, is observed at ~ 37 Å^2·monomer^{-1}. $\varepsilon_{s,max}$ is believed to correspond to the limiting value of the lateral compressibility for the completely adsorbed monolayer state. It is clear that the A/W interface is a good solvent for PCL, and that PCL forms a liquid-expanded monolayer given the magnitude of the maximum static elasticity, $\varepsilon_{s,max}$ ~ 14 mN·m^{-1}. Further compression to A < ~ 37 Å^2·monomer^{-1} could be interpreted as raising the surface energy above the threshold necessary to start desorbing some of the ester linkages.

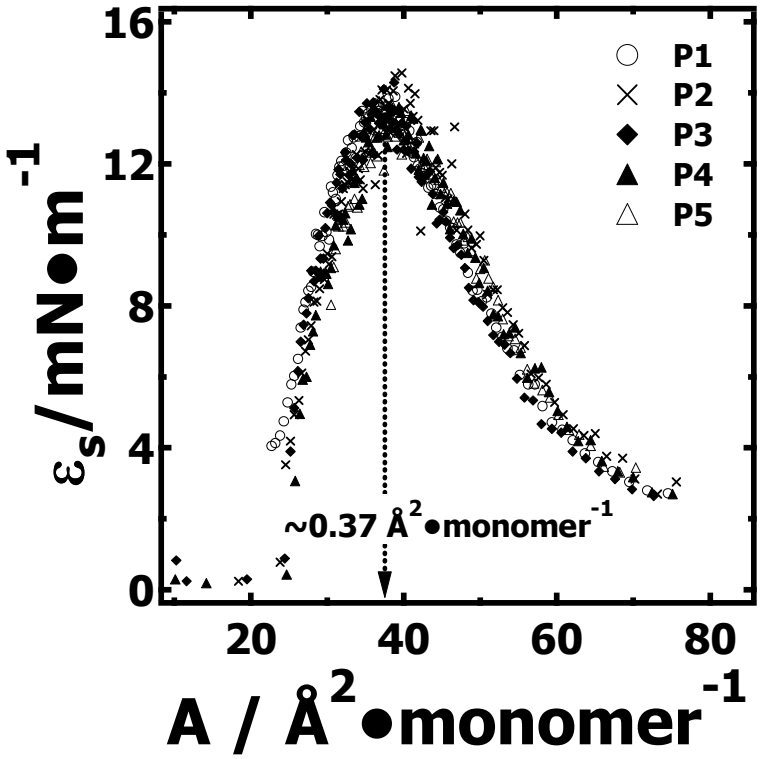

Figure 8.3. ε_s-A curves for PCL samples with different molar masses. The experiments were performed at a constant compression rate of 8 $cm^2 \cdot min^{-1}$ and T = 22.5 °C. The symbols correspond to M_w = 5.2 (P1, ○), 10 (P2, ×), 13 (P3, ♦), 15.5 (P4, ▲), and 42.8 (P5, Δ) $kg \cdot mol^{-1}$. All ε_s-A plots exhibit a maximum at A ~ 37 $Å^2 \cdot monomer^{-1}$.

8.3.3. Compression Π-A Isotherms for A ≤ ~ 37 Å^2·monomer^{-1}

Deviation from an ideal semi-dilute monolayer is observed for A ≤ ~ 37 Å^2·monomer^{-1} (Π > ~ 5.8 mN·m^{-1}). For compression of the films beyond this point, PCL monolayers start to exhibit molar mass dependent behavior as the molar mass dependent collapse pressures, Π_C, are approached. Recalling the orthorhombic unit cell of PCL (the parameters of the unit cell are a = 7.48 ± 0.02 Å, b = 4.98 ± 0.02 Å, and c = 17.26 ± 0.03 Å, respectively),[112-114] the cross-sectional area of one segment is equal to (ab)/2 = 37.2/2 = 18.6 Å^2·monomer^{-1}. By comparing this value with the value of A ~ 37 Å^2·monomer^{-1} in the vicinity of $\varepsilon_{s,max}$, it seems reasonable that all hydrophilic ester groups could be anchored to the surface with short $(CH_2)_5$ loops. A schematic depiction of idealized chain conformations for PCL at the A/W interface at different surface concentrations is shown in Figure 8.4. This configuration is particularly reasonable given the cyclic monomer from which PCL is derived. Thus, at A ~ 37 Å^2·monomer^{-1}, the surface area occupied by each repeat unit of PCL is roughly equivalent to two times the cross-sectional area of one segment in the crystalline state. Even though there is no obvious kink in the Π-A isotherm, ε_s, which is related to the slope of the Π-A isotherm by Eq. 8-3, decreases for A < ~ 37 Å^2·monomer^{-1} as seen in Figure 8.3. This drop in ε_s could be interpreted as some ester linkages leaving the surface. Furthermore, the structural relaxation in this regime could be slow since the polymer chains are firmly anchored to the water surface by hydrophilic ester linkages. Under these conditions, the compression rate could be faster than the rate of conformational changes occurring in the monolayer. As a result, the isotherm would not reveal an obvious transition such as a kink or plateau at this point.

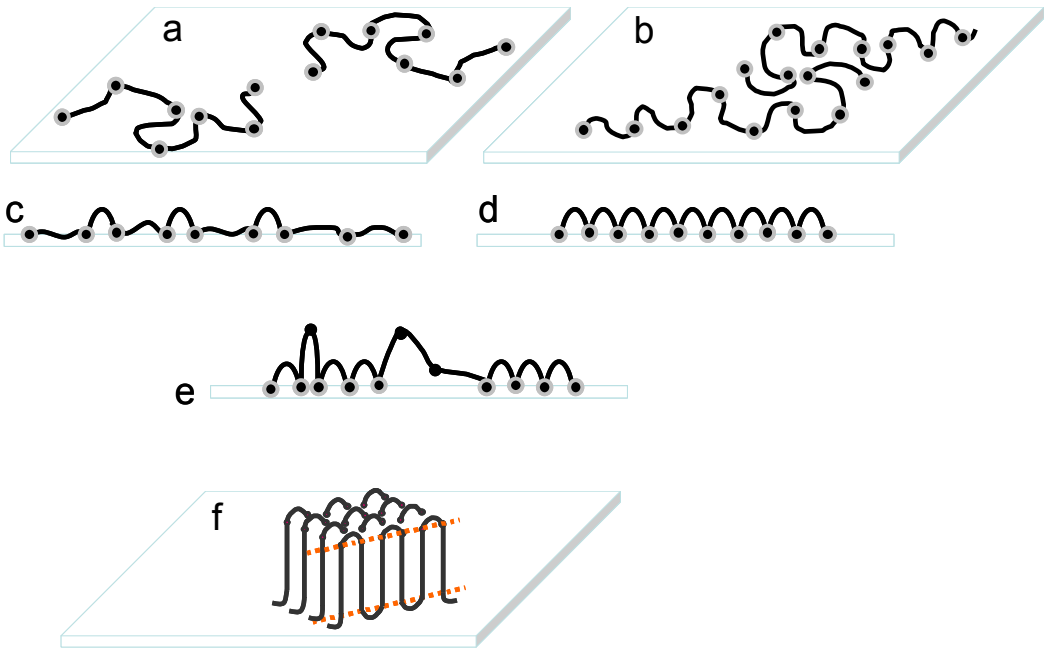

Figure 8.4. Schematic depiction of idealized chain conformations for PCL at the air/water interface at different surface concentrations: (a) A > 52 $Å^2$·$monomer^{-1}$ (top-view), (b) A ~ 52 $Å^2$·$monomer^{-1}$ (top-view), (c) 37 < A < 52 $Å^2$·$monomer^{-1}$ (side-view), (d) A ~ 37 $Å^2$·$monomer^{-1}$ (side-view), (e) A < 37 $Å^2$·$monomer^{-1}$ and before film collapse (side-view), and (f) film collapse and the formation of lamellar crystals (side-view). Upon further compression, crystals grow larger and the amorphous phases may be squeezed out of the crystallites. The black spheres represent the ester functional groups while the light coronas indicate ester groups bound to water. The connecting lines depict the methylene groups of the polymer chains.

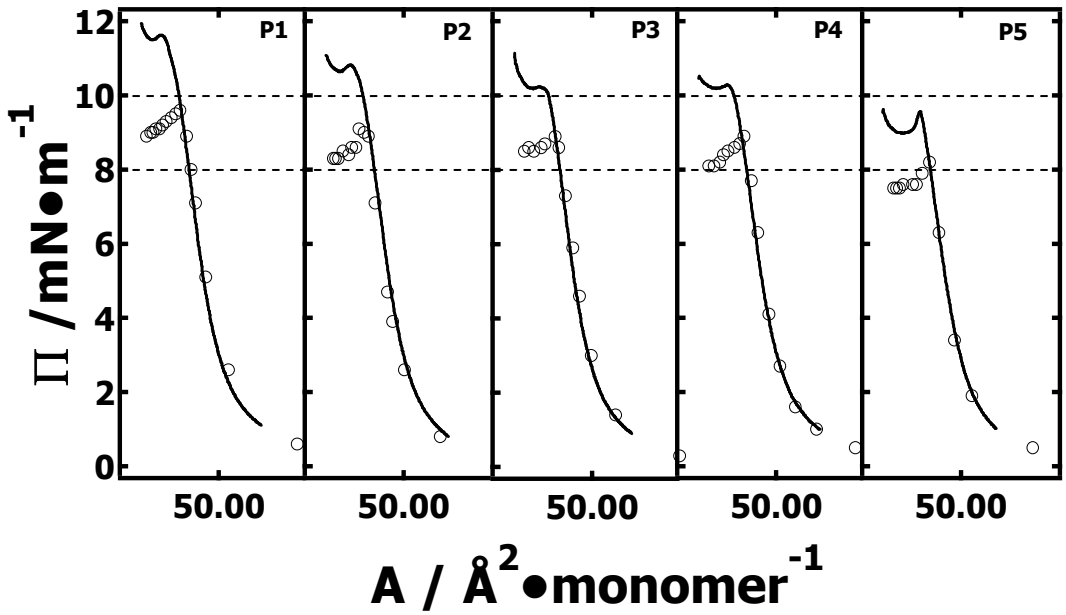

Figure 8.5. Comparisons between "equilibrium" (addition) and dynamic (compression) Π-A isotherms for PCL samples with different molar masses. P1, P2, P3, P4, and P5 correspond to M_w = 5.2, 10, 13, 15.5, and 42.8 kg·mol^{-1}, respectively. The compression isotherms (solid line) were obtained at a constant compression rate of 8 cm^2·min^{-1} and T = 22.5 °C. The circles represent successive addition data. The horizontal dashed lines at Π = 8 and 10 mN·m^{-1} are only provided to guide the eyes.

The dynamic nature of the compression isotherm is further illustrated in Figure 8.5 where comparisons between compression and successive addition isotherms are provided. Both compression and addition isotherms demonstrate molar mass dependent phase behavior in the vicinity of the collapse transition. Generally speaking, "kinks" observed in Π-A isotherms of polymers around Π_C arise from kinetic effects corresponding to the conversion of quasi-2D monolayer materials into three dimensional (3D) materials at the

A/W interface.[204, 205] As reported by Li *et al*.,[24] nucleation starts when the PCL monolayer is compressed into the supersaturated state, i.e. when Π is slightly below Π_C during constant compression experiments. In the supersaturated monolayer regime, the nucleation may be initiated at locally thicker sites since some ester linkages are already being squeezed out of the water surface for A < ~ 37 $Å^2 \cdot monomer^{-1}$. The conversion rate of "2D" material to 3D phases eventually becomes faster than the compression rate, causing Π to drop, thereby creating a noticeable "kink" in the isotherm. In constant compression experiments, the faster the overall conversion rate of the "2D" matrix to 3D materials (mainly governed by the nucleation rate), the earlier the conversion rate exceeds the compression rate (constant), and the smaller the value of Π_C. Compression isotherms (solid lines) in Figure 8.5 exhibit an increasing Π_C with decreasing PCL molar mass. This observation indicates that the nucleation rate for P1 (M_w = 5.2 $kg \cdot mol^{-1}$) could be the smallest among the five samples.

The distinct plateau regions in the compression isotherms are related to the growth of a 3D phase, PCL crystals (to be shown shortly).[24] On the plateau, the conversion rate matches the compression rate, i.e. the decrease in A is compensated by the conversion of "2D" monolayer material to 3D phases (mainly contributed by PCL crystallization). Since the nucleation and growth of crystals in bulk depends on molar mass, it is not surprising that the isotherms of PCL around the collapse transition and subsequent plateau are molar mass dependent. In bulk systems, molar mass affects the degree of undercooling ($\Delta T = T_m^0 - T_x$) because the equilibrium melting temperature, T_m^0, is molar mass dependent. Previous studies of spherulitic growth in supercooled PCL melts indicate that T_m^0 increases with increasing chain length until a plateau is observed.[24] This

behavior is explained by decreases in fractional free volume with increasing molar mass. Hence, polymers with higher molar mass exhibit higher T_m^0, and greater degrees of undercooling for a fixed crystallization temperature, T_x (in this case 22.5 ^oC). As the nucleation rate increases with an increasing degree of undercooling, the nucleation rate also increases with increasing molar mass. Thus, decreases in Π_C with increasing molar mass demonstrated in Figure 8.5 are consistent with a greater nucleation rate for higher molar mass compounds.

Addition isotherms (circles in Figure 8.5) were also used to explore the molar mass dependent collapse behavior of a PCL monolayer under "equilibrium" conditions. As seen in Figure 8.5, no obvious differences are observed for Π-A isotherms obtained from compression and addition experiments in the semi-dilute monolayer regime within experimental errors (±0.2 $mN \cdot m^{-1}$). In contrast, allowing equilibration during the addition experiment at $\Pi \geq \sim 8$ $mN \cdot m^{-1}$, where nucleation can occur during compression experiments, causes Π to relax to lower values. This observation indicates that in the metastable region (~ 8 $mN \cdot m^{-1} < \Pi < \Pi_C$, the nucleation and growth of crystals is energetically favorable.[24] The decrease of the "equilibrium" Π_C observed in successive addition experiments with increasing molar mass parallels the dynamic Π_C behavior observed in compression experiments.

Unlike the nucleation process from quiescent melt or solution, in which the energy barrier for the formation of a nucleus is overcome if there is a sufficient degree of undercooling,[115] nucleation at the A/W interface could also be influenced by the mechanism of film collapse, i.e. the chain dynamics upon compression. For example, Π_C values can also be affected by the time scale for structural relaxation, which is faster for

polymer chains with smaller molar masses. In addition, any prior impurity, polydispersity, spreading method, solution concentration, solvent purity, or even factors in the synthetic process such as functional end groups could also affect the nucleation process in PCL monolayers at the A/W interface. Even though all of these factors may influence Π_C, it is our belief that nucleation from PCL monolayers at the A/W interface is mainly controlled by the degree of undercooling as reflected by Π_C.

8.3.4. Molar Mass Dependent Morphologies for PCL Crystals Grown During Compression

At the A/W interface, the unique chain dynamics observed upon compression, the confinement of mass diffusion to "2D", and the essentially instantaneous dissipation of heat evolved from the crystallizing monolayer to the subphase may lead to crystal features that are different from those formed in quiescent melt or solution, and even spincoated films. Figure 8.6 contains BAM images obtained at different A values during the compression of PCL Langmuir films with different molar masses. The appearance of bright domains is attributed to the formation of 3D crystals. The nucleation event for these crystals corresponds to the collapse of the monolayer in the metastable state, whereby additional carbonyl groups pull away from the surface and form folded chain lamellar crystals.[31] Because of the greater rotational freedom of the ester linkages around the polymer backbone, the ester groups could be forming hairpin turns allowing the chain to fold back and forth in a similar fashion to the folded chain structure of polyethylene single crystals formed from dilute solution.[115] For compression past Π_C, the polymer chains start to rapidly deposit onto the growing front of the newly formed 3D nuclei. Within the plateau regions of the Π-A isotherms for P1- P4, obvious changes in the

number density of crystals have not been observed during compression relative to the number density of crystals observed around the collapse points. Although a distribution of crystal sizes are observed for a given molar mass by BAM (as seen in Figure 8.6), most of the crystals have similar sizes suggesting that nuclei formed around the "kink" in the Π-A isotherm are mainly responsible for the conversion of "2D" materials to a 3D phase in the plateau region. Moreover, crystal growth in the plateau regime is energetically more favorable as primary nucleation requires a larger specific area than secondary nucleation on the surface of existing nuclei, i.e. the energy barrier for primary nucleation is higher than for secondary nucleation.

As pointed out by Chen *et al*. the competition between lower segmental mobility and a greater degree of undercooling with increasing molar mass produces a maximum average growth rate at intermediate molar mass for PCL crystal growth in bulk melts.[2] Over the experimental time scale, the size of the crystals for the five PCL samples grown at the A/W interface also exhibits a maximum growth rate for P2. The P1 sample, with the lowest molar mass, has the smallest degree of undercooling. The primary nucleation rate for P1 could be the lowest as reflected by Π_C in Figure 8.1. Meanwhile, the higher energy growth fronts of the stable P1 nuclei are less conducive for crystal growth, even though the P1 sample possesses the greatest chain mobility, a factor that when considered alone would favor easy deposition of new polymer chains from the "surrounding monolayer" onto growing crystal faces (secondary nucleation) relative to P2 through P5. The overall effects of these factors result in a smaller growth rate and subsequently smaller crystal sizes for P1 relative to P2. At the other extreme, the highest molar mass P5 sample crystallizes with the greatest degree of undercooling, suggesting P5 has the highest

primary nucleation rate among all five samples since ΔT has a more significant effect on the primary nucleation rate than on the subsequent growth process which is dominated by secondary nucleation.[2] Furthermore, the P5 sample also has the slowest diffusion coefficient which could hinder the deposition of polymer chains from the surrounding monolayer onto the growing crystal (secondary nucleation). As a result, the primary and secondary nucleation rates could be comparable. Such a case would be consistent with the observation that the P5 sample has the largest number of nuclei and smallest crystal sizes for comparable crystallization times.

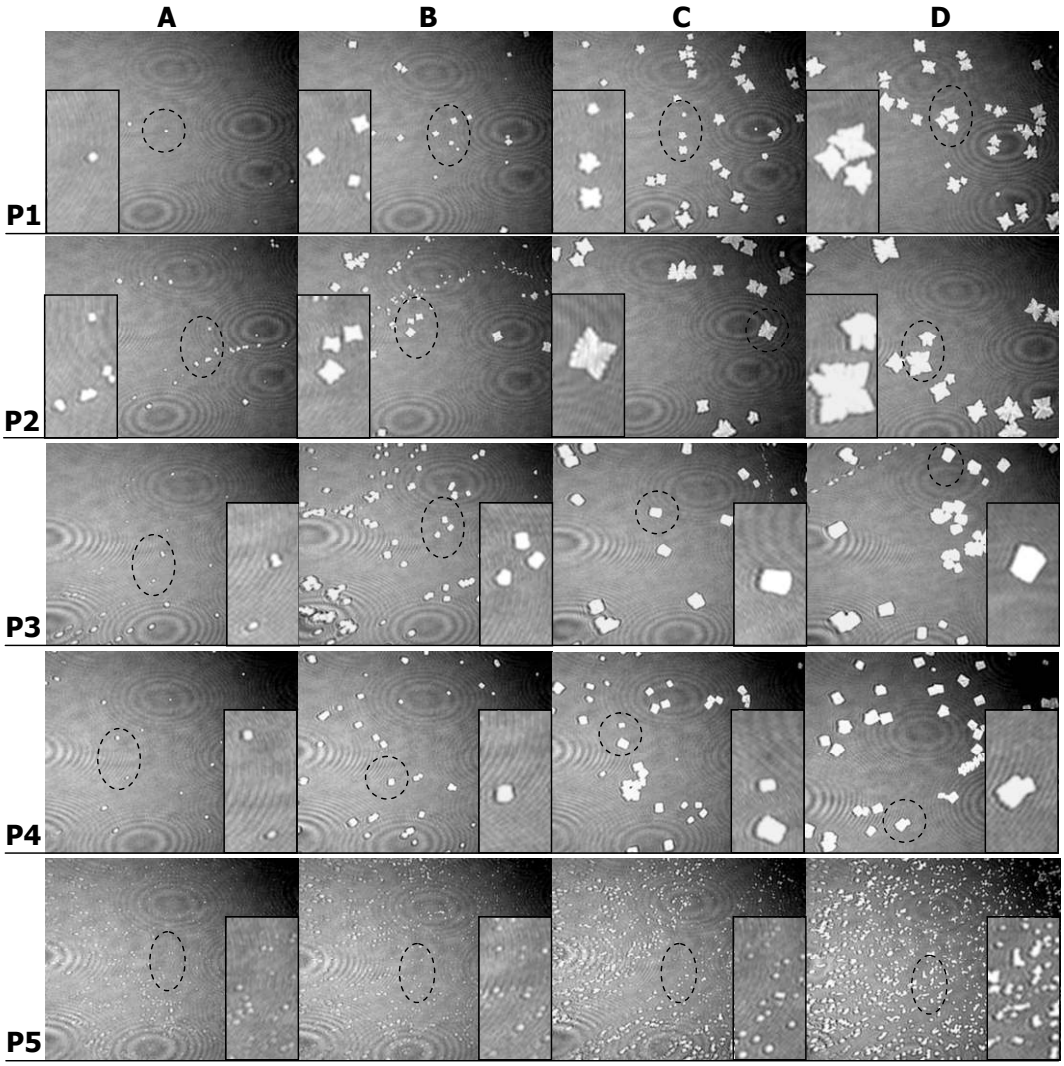

Figure 8.6. BAM images obtained during film compression for PCL samples with different molar masses. The experiments were performed at a constant compression rate of 8 $cm^2 \cdot min^{-1}$ and T = 22.5 °C. P1, P2, P3, P4, and P5 correspond to M_w = 5.2, 10, 13, 15.5, and 42.8 $kg \cdot mol^{-1}$, respectively. The BAM images (A→D) correspond to the labeled arrows on the Π-A isotherm in Figure 8.1 (A = 22 ~ 23, B = 18 ~ 19, C = 13 ~ 14, and D = 11 ~ 12 $Å^2 \cdot monomer^{-1}$). The areas circled in the 4.4 × 3.5 mm^2 BAM images were magnified and displayed as 0.5×1.0 mm^2 insets.

Looking at the morphological details of BAM images for P1(A)→(D) in Figures 8.6, during the early stages of compression, BAM images show the first 3D domains appear around A ~ 22 $Å^2$·$monomer^{-1}$. Upon further compression, individual domains grow larger and take on a "butterfly" shape. The crystal morphologies for P1(B)→(D) are quite similar to those for P2 crystals as seen in images P2(B)→(D). The "butterfly" shapes are consistent with diffusion-limited growth of PCL crystals in these two samples.[31] For P3 and P4 samples, distorted rectangular morphologies are observed, suggesting that four {110} faces could become more fully developed in comparison to P1 and P2 samples. BAM images for the P5 sample are also shown in Figure 8.6, P5(A)→(D). The area fraction occupied by bright domains increases upon compression, even though the crystallites are so small that the growth of individual crystals cannot easily be followed by BAM.

8.3.5. Estimation of Average Growth Rates

As shown in Figure 8.6, the qualitative trend of crystals grown upon compression and the molar mass dependent crystal sizes are clearly revealed by BAM at comparable A values. Hence, it is desirable to estimate the overall growth rates from the BAM images. Unfortunately, this is not trivial and several approximations need to be made. Unlike measurements of growth rates from spherulites in bulk, where the radius of a single spherulite can be measured by optical or atomic force microscopy until it impinges upon its neighbors, crystals at the A/W interface are subject to flow. This complication means that it is impossible to keep a crystal in the BAM's field of view over the crystal's entire lifetime. A second complication is that nucleation does not start at the same time for all crystals leading to a size distribution in any given BAM image. This complication is

avoided in bulk measurements through the study of the same spherulite over its lifetime. Finally, the crystals in Figure 8.6 are clearly anisotropic. To overcome these problems, the following procedure is used to estimate the average growth rates: (1) First, the length of the longest tip to tip distance for a given crystal serves as the linear dimension; (2) Typically 6 to 12 crystals with representative sizes in a given image are measured. The exception to this is immediately after nucleation starts where as few as 2 to 4 crystals, i.e. all of the crystals in the field of view, are measured. Crystals that were obviously much smaller or larger than average were not included. This cut-off is somewhat arbitrary, however, it is required so that measured crystals represent crystals that underwent nucleation at a similar time in each BAM image; and (3) The linear dimensions were then averaged and are plotted in Figure 8.7 as a function of the crystallization time with one standard deviation error bars. The time at which the "kink" occurs (collapse point) was considered to be the initial time, t_0. The time for each BAM image captured during the plateau region is considered as t. The crystallization time, t_x, for the crystals measured in these BAM images was computed as $t_x = t - t_0$. While the growth rates obtained from this procedure may not be ideal, it is the best that can be done at this time and the subsequent discussion is offered in light of these assumptions.

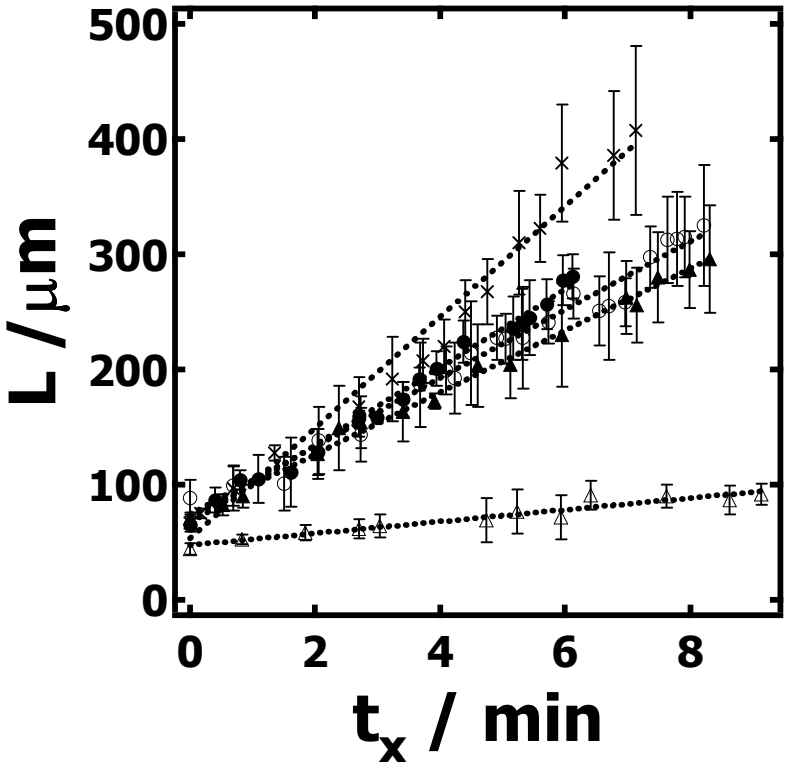

Figure 8.7. Average tip-to-tip length, L, versus crystallization time, t_x, for PCL samples with various molar masses, M_w = 5.2 (P1, ○), 10 (P2, ×), 13 (P3, ○), 15.5 (P4, ▲), and 42.8 (P5, Δ) kg·mol^{-1}. Dotted lines represent the linear fit used to estimate the average growth rate. Error bars on the individual data points represent ± one standard deviation following the procedure outlined in the text.

In Figure 8.7, t_x is restricted to the plateau region of the isotherm to ensure Π is more or less constant. Meanwhile, t_x is very short in comparison with PCL crystallization in spincoated films.[9] The experimental trends observed in Figure 8.7, along with the absence of any strong theoretical reason for assuming non-linear growth rates during such a short period of growth, leads to the assumption of linear growth rates for the subsequent

discussion.[2] The slopes from the empirical linear fits in Figure 8.6, $G = dL/dt_x$, then yield the average crystal growth rates. These values are summarized in Table 8.1. One feature of Figure 8.7 and Table 8.1 is quite striking, the P2 (M_w = 10 kg·mol^{-1}) sample exhibits the largest growth rate. This feature is particularly interesting when one considers bulk crystallization rates for PCL melts.[2]

Table 8.1. Average growth rates for PCL monolayers at the A/W interface.

#	M_w kg·mol^{-1}	M_n kg·mol^{-1}	ln X_n	G μm·min^{-1}	G μm·sec^{-1}	ln G ln(G/μm·sec^{-1})
P1	5.2	3.5	3.42	33.8±0.9	0.56±0.02	-0.57±0.03
P2	10	8	4.25	47.9±2.6	0.80±0.05	-0.23±0.06
P3	13	11	4.57	29.6±1.0	0.49±0.02	-0.71±0.04
P4	15.5	13	4.74	26.9+0.6	0.45±0.01	-0.80±0.03
P5	42.8	36	5.76	5.1±0.5	0.09±0.01	-2.47±0.10

Error bars represent ± one standard deviation.

Figure 8.8 shows Chen *et al.*'s growth rate data plotted as a function of the number average degree of polymerization (X_n) for different temperatures on a *ln-ln* scale.[2] Chen *et al.*'s data clearly show G exhibits a maximum value for intermediate molar mass at each temperature. The G values from Table 8.1 obtained at a temperature of 22.5 °C for Langmuir films of PCL with various molar masses are also plotted on Figure 8.8. It is interesting to note that the magnitude of the G values from the Langmuir films is comparable to bulk data at smaller degrees of undercooling and that the molar mass where the maximum G value occurs is comparable to the bulk systems. These observations indicate that PCL crystallization is less favorable at the A/W interface than in bulk, possibly because of interactions with water. Nonetheless, the growth rates at the

A/W interface are much faster than for PCL crystallization in spincoated films on silicon substrates at thicknesses < 15 nm.[9] Hence, the slower growth rate at the A/W interface relative to bulk systems could also be caused by a confinement effect, where mass transport to the growing crystal front is hindered.

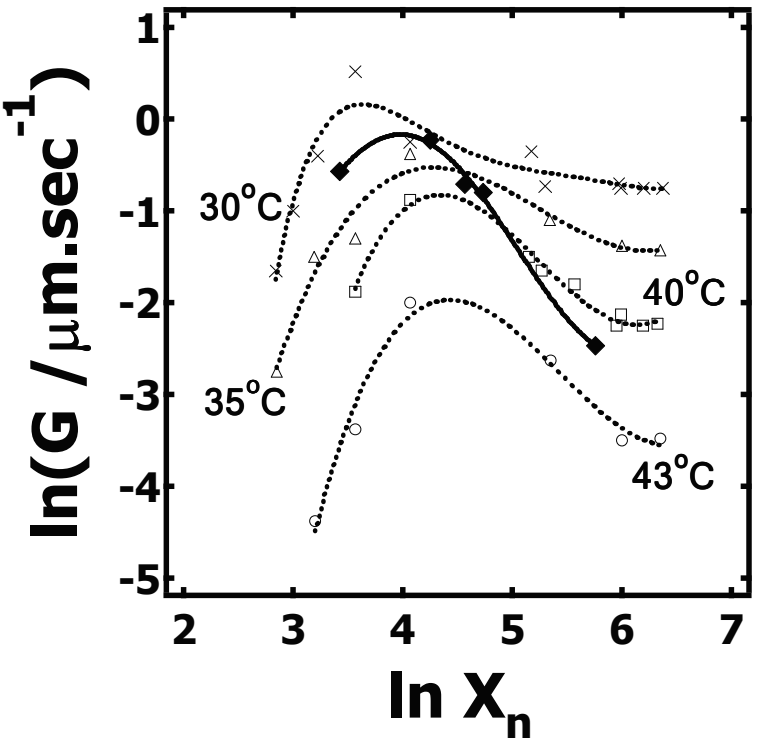

Figure 8.8. Growth rate vs. degree of polymerization for PCL. Both spherulitic growth in melts[2] and crystallization in Langmuir monolayers exhibit a maximum growth rate. Literature data for the melts correspond to temperatures of (×) 30 °C, (Δ) 35 °C, (□) 40 °C, and (○) 43 °C.[2] Symbols (♦) indicate the average growth rate data obtained at 22.5 °C in Langmuir monolayers. The dotted and solid lines in the figure are provided to guide the eye through the trends.

8.3.6. Π-A Isotherm and Morphology Studies of Melting PCL Crystals During Expansion

Figure 8.9 shows Π-A isotherms of PCL with different molar masses obtained during expansion experiments at a constant expansion rate of 8 $cm^2 \cdot min^{-1}$ and T = 22.5 °C. Expansion of the film started from ~5.7 $Å^2 \cdot monomer^{-1}$ following the compression step shown in Figure 8.1. During the expansion process, the non-equilibrium crystals grown during film compression start to undergo conformational relaxation rather than instantaneous melting and respreading at the A/W interface. The surface pressure drops very quickly during the initial stages of the expansion process. After the rapid drop in Π, a plateau region forms in the expansion isotherm. In the plateau region, the crystals start to melt, i.e. the polymer chains peel away from the crystals and start to respread on the surface. As both steps (structural relaxation and respreading) of the melting process are transport limited, a strong molar mass dependence is expected and observed in the expansion isotherms. As seen in Figure 8.9, the plateau Π values dramatically decrease with increasing molar mass from P1 to P2, indicating slower detachment of molecules from the edges of the crystals for the higher molar mass samples. The critical surface pressure for the onset of crystal melting (Π_m) during expansion was defined as the y-intercept (Π-intercept) of the tangent line for the plateau regime in the expansion isotherm. Thus, the critical surface tension can be estimated as $\gamma_C = 72 - \Pi_m$. The inset of Figure 8.9 shows a plot of γ_C vs. M_w. As M_w increases, γ_C rises sharply before plateauing. In bulk systems, the free volume dependent T_m^0 exhibits a similar trend with respect to

molar mass. Here, γ_C can be regarded as the analogous property to T_m^0 for Langmuir films at the A/W interface.

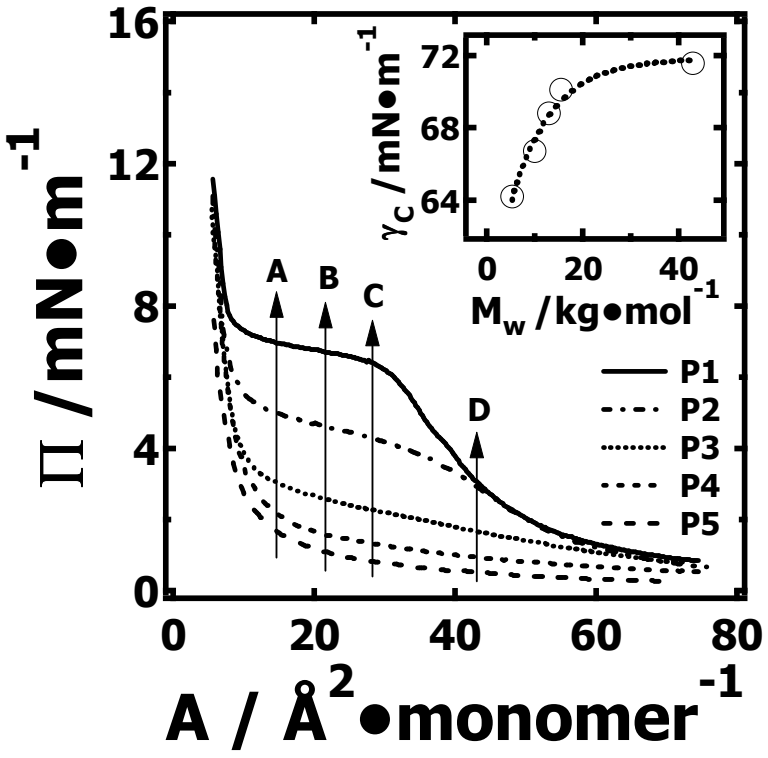

Figure 8.9. Expansion ∏-A isotherms for PCL samples with different molar masses. The experiments were performed at a constant expansion rate of 8 $cm^2 \cdot min^{-1}$ and T = 22.5 °C. P1, P2, P3, P4, and P5 correspond to M_w = 5.2, 10, 13, 15.5, and 42.8 $kg \cdot mol^{-1}$, respectively. The letters on the graph correspond to the A values where the BAM images in Figure 8.10 were taken. The starting point for each expansion curve was the end of the compression isotherms in Figure 8.1. The inset figure is the critical surface tension for the onset of the plateau during expansion, γ_C, plotted against M_w. The dotted line in the inset only indicates the trend.

By utilizing BAM, the melting of the crystals during expansion can be directly followed as seen in Figure 8.10. Images P1(A)→(D) in Figure 8.10 indicate that the crystals of P1 start to melt at the early stage of the plateau region, A ~ 14 $Å^2 \cdot monomer^{-1}$, from the four in-plane faces of the 3D square crystals (noting that the thickness, ~ 8 nm,[24] is much smaller than the in-plane dimension). As the surface concentration decreases, the cross-like principle axes appear as seen in images P1(B)→(C) in Figure 8.10, and all the bright domains become smaller and smaller and finally disappear as shown in image P1(D). Sample P2 exhibits a similar melting process and dendritic crystals are also observed during expansion of the film. All of the bright domains disappear at larger A (smaller Π) than P1. Combined with the result of the Π-A isotherms shown in Figure 8.9, the plateau regions can be correlated to the transport processes associated with going from 3D crystals back to a "2D" monolayer state, where the polymer chains continuously peel off from the crystals to compensate for the decrease in Π that resulted from the expansion of the barriers. The plateau Π values for P1 and P2 indicate that higher molar mass PCL samples are less mobile than the lower molar mass samples at the A/W interface. Meanwhile, the lower molar mass samples also have greater instability at the crystal fronts, resulting in crystals that respread faster during expansion. After the plateau region, most of the 3D material has been transferred back onto the water surface, and Π again drops in response to increasing trough area. For sample P3 and P4, no regular cross-like principal axes were observed by BAM during the melting process as seen in Figure 8.10. Moreover, some bright domains can still be observed (not shown) for P3 and P4 even after the trough area was expanded back to the initial (maximum) trough area. For the P5 sample, bright domains can still be observed (not shown) at the

maximum trough area as well. The surface morphologies observed are consistent with the expansion isotherms in Figure 8.9 since the Π-A isotherms do not show an obvious end to the plateau regions (crystal melting) and have greater hysteresis for P3, P4, and P5. Collectively, this behavior suggests that the complete melting of crystals for high molar mass PCL may not be possible during film expansion at the A/W interface. In addition, even though no bright domains were observed by BAM after expanding the barriers to the maximum trough area for the P2 sample, a 2nd compression step does not retrace the initial compression step because of long lived 3D structures that can serve as nucleation centers and lead to different crystal morphologies during the 2nd compression step.[24]

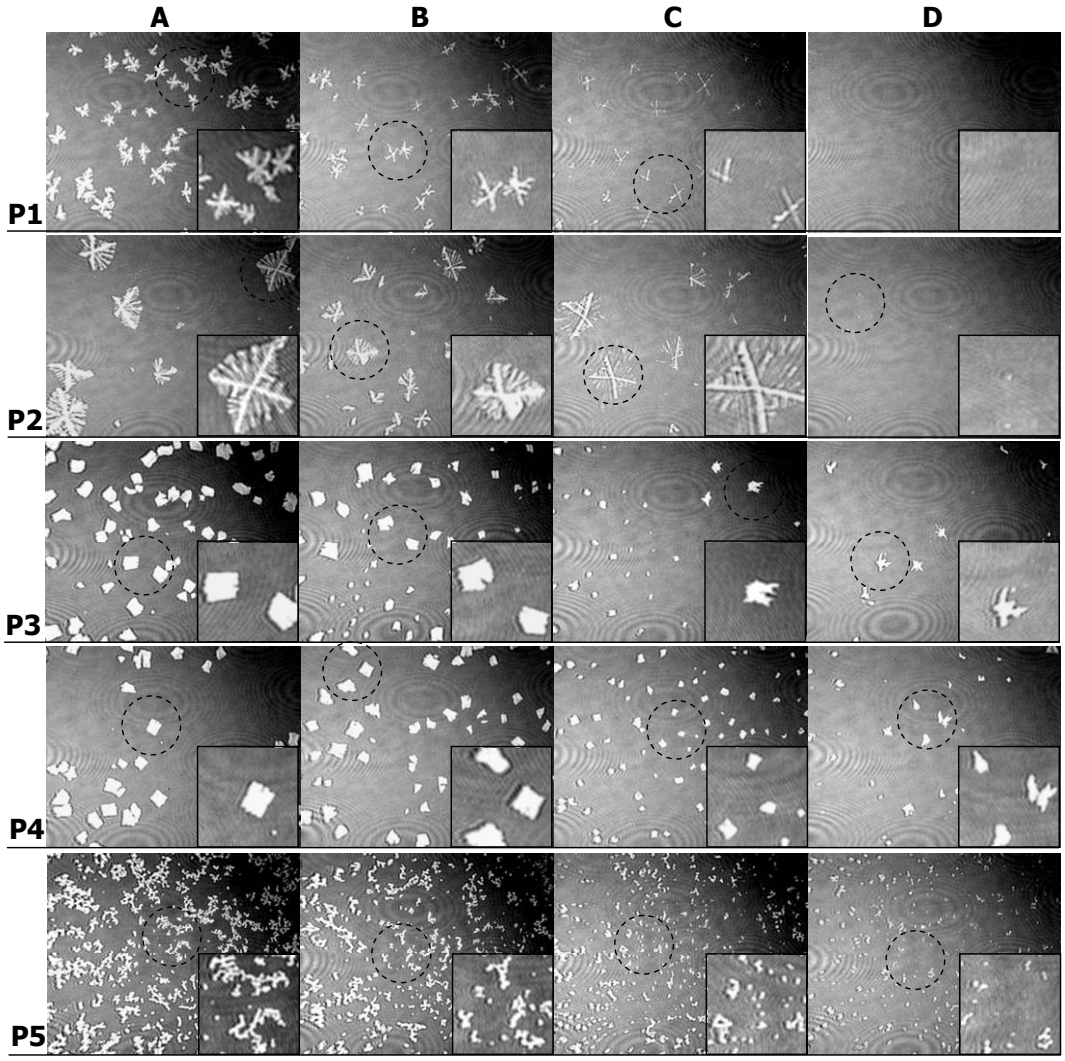

Figure 8.10. BAM images for PCL samples with different molar masses obtained during film expansion. The experiments were performed at T = 22.5 °C and an expansion rate of 8 $cm^2 \cdot min^{-1}$. P1, P2, P3, P4, and P5 correspond to M_w = 5.2, 10, 13, 15.5, and 42.8 $kg \cdot mol^{-1}$, respectively. The BAM images (A→D) correspond to the labeled points on the Π-A expansion isotherm in Figure 8.9 (A = 14 ~ 15, B = 21 ~ 22, C = 28 ~ 29, and D = 42 ~ 43 $Å^2 \cdot monomer^{-1}$). Bright domains correspond to the morphologies of crystals during the melting process. The area circled in the 4.4 × 3.5 mm^2 BAM images were magnified and displayed as 0.8 × 0.8 mm^2 insets.

8.4. Conclusions

In summary, both Π-A isotherm and morphological studies by BAM indicate that the surface pressure induced nucleation and growth of PCL crystals in Langmuir monolayers at the A/W interface is affected by molar mass. The nucleation of PCL crystals starts from a supersaturated monolayer regime where the molar mass dependent Π_C values from compression isotherms correlate with the tendency of the various PCL samples to form 3D critical nuclei. The molar mass dependent growth of PCL crystals are further confirmed by growth rate data estimated from a series of BAM images obtained during the compression experiments. A maximum growth rate at an intermediate molar mass is observed. The maximum growth rate is believed to represent a competition between lower segmental mobility and a greater degree of undercooling with increasing molar mass. The morphological study is particularly interesting, as it shows diffusion-limited growth for the lower molar mass PCL samples and dendritic morphologies are clearly observed during expansion of the films. In contrast, for high molar mass samples, the diffusion of polymer chains during compression inhibits crystal growth; while the greater degree of undercooling favors nucleation leading to more and smaller crystals. Hence, the present study is a significant supplement to the field of traditional polymer crystallization. In particular, Π-induced PCL crystallization can be used as a model system to study the effects of molar mass on crystal morphologies and growth rates in constrained "2D" geometries.